

Communication

Potassium 6-Oxo-7,13,16,22-tetraazatetracyclo[12.6.2.1^{8,12}.0^{17,21}]tricoso-1(20),8(23),9,11,14,16,18,21-octaen-2-yne-15-carboxylate

Camille Blouet ¹, Stéphanie Letast ¹, Thomas Robert ^{2,3}, Stéphane Bach ^{2,3,4} , Noël Pinaud ⁵ , Nicolas Joubert ¹ , Marie-Claude Viaud-Massuard ¹, Jean Guillon ⁶ , Cédric Logé ⁷  and Caroline Denevault-Sabourin ^{1,*} 

- ¹ Research Center for Respiratory Diseases (CEPR), Team: "Proteolytic Mechanisms in Inflammation", University of Tours, INSERM, UMR 1100, F-37032 Tours, France
- ² Integrative Biology of Marine Models Laboratory (LBI2M), Sorbonne University, CNRS, UMR8227, F-29680 Roscoff, France
- ³ Kinase Inhibitor Specialized Screening facility (KISSf), Sorbonne University, CNRS, FR2424, F-29680 Roscoff, France
- ⁴ Centre of Excellence for Pharmaceutical Sciences, North-West University, Private Bag X6001, Potchefstroom 2520, South Africa
- ⁵ Institut des Sciences Moléculaires (ISM), University of Bordeaux, CNRS, UMR 5255, F-33405 Talence, France
- ⁶ ARNA Laboratory, University of Bordeaux, INSERM U12132-UMR CNRS 5320, F-33076 Bordeaux, France
- ⁷ Department of Medicinal Chemistry, IICIMED-UR1155, IRS2, Nantes University, F-44200 Nantes, France
- * Correspondence: caroline.denevault@univ-tours.fr; Tel.: +33-2-47-36-72-31

Abstract: Potassium 6-oxo-7,13,16,22-tetraazatetracyclo[12.6.2.1^{8,12}.0^{17,21}]tricoso-1(20),8(23),9,11,14,16,18,21-octaen-2-yne-15-carboxylate was synthesized through a multi-step pathway, starting from commercially available 3-iodo-1,2-phenylenediamine. Structure characterization of this new substituted macrocyclic quinoxaline compound was achieved using ¹H NMR, ¹³C NMR, and HRMS spectral analysis. This new macrocyclic derivative demonstrated submicromolar potency on both Pim-1 and Pim-2 isoforms, with an interesting selectivity profile against a selected panel of human kinases.



Citation: Blouet, C.; Letast, S.; Robert, T.; Bach, S.; Pinaud, N.; Joubert, N.; Viaud-Massuard, M.-C.; Guillon, J.; Logé, C.; Denevault-Sabourin, C. Potassium 6-Oxo-7,13,16,22-tetraazatetracyclo[12.6.2.1^{8,12}.0^{17,21}]tricoso-1(20),8(23),9,11,14,16,18,21-octaen-2-yne-15-carboxylate. *Molbank* **2023**, *2023*, M1735. <https://doi.org/10.3390/M1735>

Academic Editor: Luke R. Odell

Received: 30 August 2023

Revised: 26 September 2023

Accepted: 7 October 2023

Published: 9 October 2023



Copyright: © 2023 by the authors. Licensee MDPI, Basel, Switzerland. This article is an open access article distributed under the terms and conditions of the Creative Commons Attribution (CC BY) license (<https://creativecommons.org/licenses/by/4.0/>).

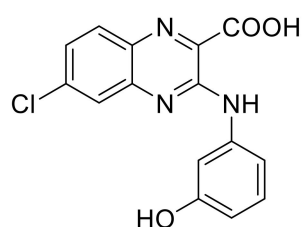
Keywords: macrocycle; quinoxaline; Pim kinases; kinase inhibitor

1. Introduction

Pim (Provirus Integration site for Moloney murine leukemia virus) kinases are a family of three constitutively active proto-oncogenic serine/threonine protein kinases (Pim-1, Pim-2 and Pim-3), regulating various cellular processes, including cell proliferation, survival and differentiation [1–4]. Pim kinases are implicated in oncogenesis, particularly in tumor progression and metastasis, and are considered as important drivers of chemotherapy resistance [5]. Thus, these kinases are overexpressed in a large variety of tumors, with differences in their expression pattern according to the cancer type. Thereby, while Pim-1 and Pim-2 are commonly up-regulated in hematopoietic cancers [6–10], Pim-3 is mostly over-expressed in some solid cancers (e.g., prostate cancers) [11]. Finally, mice deficient for all Pim kinases displayed mild phenotypic modifications, including reduced body size and impaired responses to hematopoietic growth factors [12,13], demonstrating the interest of targeting these kinases in oncology. Moreover, crystal structures of Pim-1 and Pim-2 revealed unique particularities in comparison to others kinases, which can be exploited to develop selective Pim inhibitors [14,15].

In this context, and in the course of our drug discovery program on the development of new targeted antileukemic treatments, we previously identified the new quinoxaline lead compound **1**, acting as a submicromolar dual Pim1/2 inhibitor (IC₅₀ of 130 nM and 170 nM, on Pim-1 and Pim-2, respectively) (Figure 1), but also displaying micromolar inhibition of DYRK1A and GSK3β off-target mammalian kinases [16]. In the light of these results, we decided to prepare optimized analogues of compound **1**, with an improved

selectivity profile. Thus, taking into account our experience on the structure-activity relationships (SAR) in our previously described quinoxaline derivatives series [16,17], we used the quinoxaline-2-carboxylic acid scaffold as a template for the design and the synthesis of a new macrocyclic compound. SAR and molecular modeling studies highlighted the crucial role of the carboxylic acid moiety in position two for the Pim kinase inhibitory activity, establishing a key salt bridge with the catalytic lysine residue of Pim1/2 kinases at physiological pH. Moreover, macrocycles have been emerging as a valuable class of pharmacological agents over the past decade. Indeed, macrocyclization allows restriction of the conformational freedom observed in small molecules, permitting them to optimize affinity and selectivity [18], and macrocyclic kinase inhibitors have reached advanced clinical trial, particularly in oncology [19,20]. In 2021, the Food and Drug Administration approved lorlatinib, the first macrocyclic kinase inhibitor in metastatic anaplastic lymphoma kinase (ALK)-positive non-small cell lung cancer. Here, we report the synthesis and structural identification of the potassium 6-oxo-7,13,16,22-tetraazatetracyclo[12.6.2.1^{8,12}.0^{17,21}]tricoso-1(20),8(23),9,11,14,16,18,21-octaen-2-yne-15-carboxylate **8**. This original macrocyclic quinoxaline **8** was further evaluated on human Pim-1 and Pim-2 kinases and on a selected panel of human protein kinases, to determine its selectivity profile.



Lead compound 1

Pim-1 IC₅₀ = 130 nM

Pim-2 IC₅₀ = 170 nM

Figure 1. Chemical structure of lead compound 1.

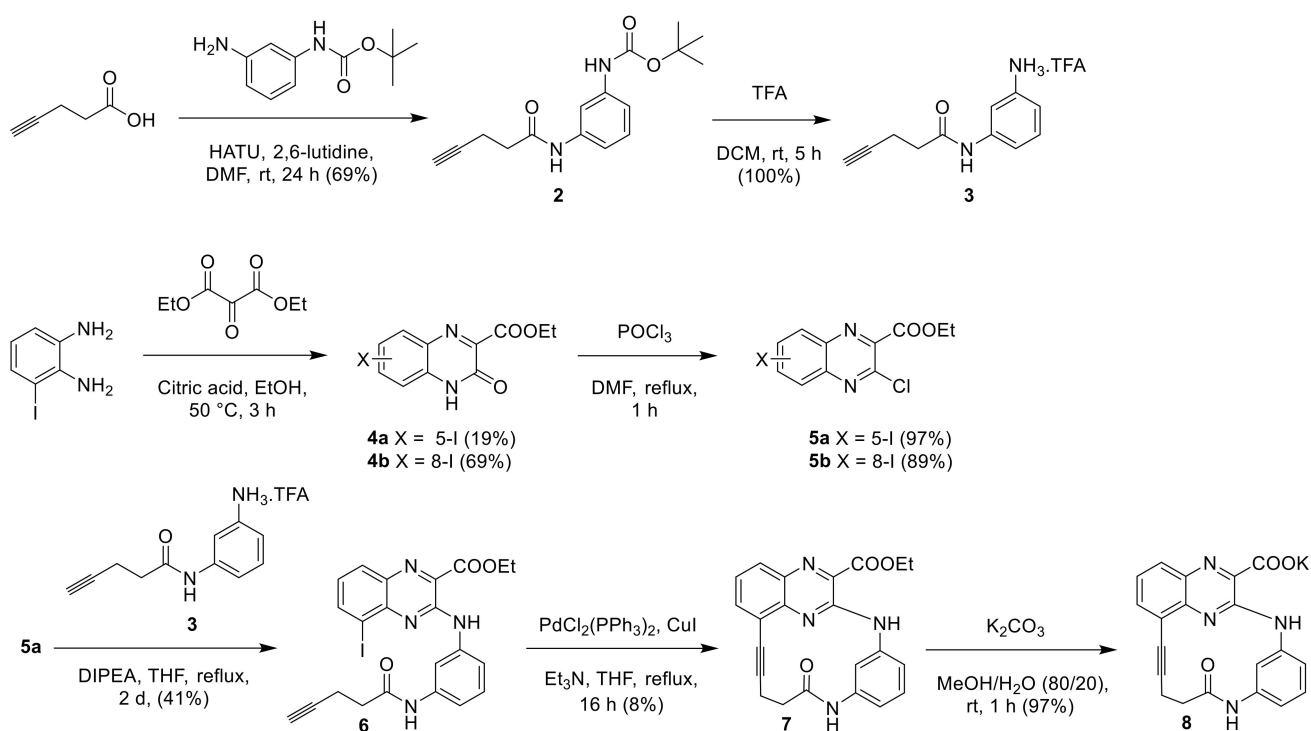
2. Results and Discussion

2.1. Potassium 6-Oxo-7,13,16,22-tetraazatetracyclo[12.6.2.1^{8,12}.0^{17,21}]tricoso-1(20),8(23),9,11,14,16,18,21-octaen-2-yne-15-carboxylate

The synthesis of the potassium 6-oxo-7,13,16,22-tetraazatetracyclo[12.6.2.1^{8,12}.0^{17,21}]tricoso-1(20),8(23),9,11,14,16,18,21-octaen-2-yne-15-carboxylate **8** was performed as described in Scheme 1.

First, intermediate **3** was synthesized in two steps. The peptide coupling reaction between commercially available pent-4-ynoic acid and *tert*-butyl (3-aminophenyl)carbamate in *N,N*-dimethylformamide (DMF), using 1-[Bis(dimethylamino)methylene]-1*H*-1,2,3-triazolo[4,5-*b*]pyridinium 3-oxid hexafluorophosphate (HATU) and 2,6-lutidine [21], gave the carbamate intermediate **2**, which was then deprotected, using trifluoroacetic acid (TFA) [22] to provide the attempted trifluoroacetic salt **3**.

The preparation of 3-chloro-5-iodoquinoxaline key intermediate **5a** was then achieved in two steps according to the literature procedures [16,17,23,24]. Briefly, commercial 3-iodo-1,2-phenylenediamine was condensed with diethyl 2-oxomalonate, in ethanol, using citric acid as catalyst [23] to give ester **4a**, which was separated from its 8-iodo isomer **4b** by silica column chromatography. Chlorination in position 3 of esters **4a** and **4b** was realized, using DMF as a catalyst, in refluxing phosphorous oxychloride [24] to give the corresponding esters **5a** and **5b**. Intermediate **5b**, in contrast with its isomer **5a**, gave a yellow single crystal, which was used for the 3D structural determination by X-ray crystallography (Figure 2), to identify the position of the iodo group on the quinoxaline scaffold in the solid state of this isomer, confirming the structure of each isomer.



Scheme 1. Synthesis of Potassium 6-oxo-7,13,16,22-tetraazatetracyclo[12.6.2.1^{8,12}.0^{17,21}]tricoso-1(20),8(23),9,11,14,16,18,21-octaen-2-yne-15-carboxylate (**8**).

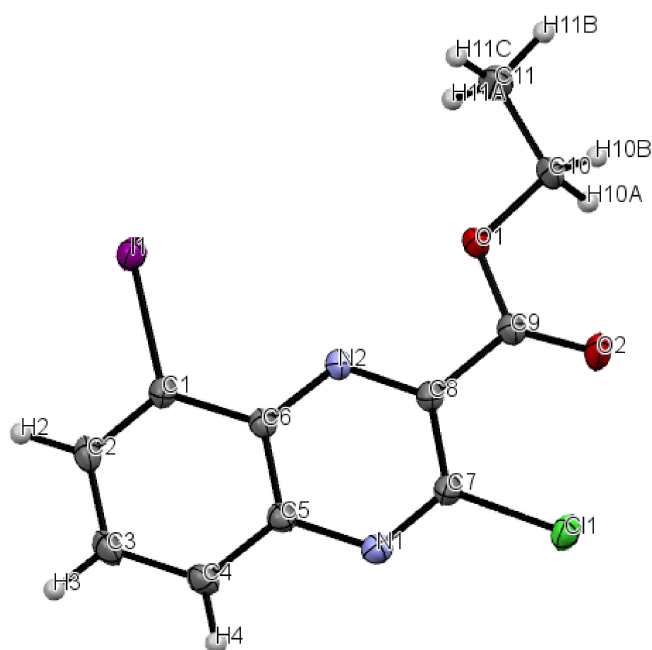


Figure 2. The ORTEP (Oak Ridge Thermal Ellipsoid Plot) drawing of ethyl 3-chloro-8-iodoquinoxaline-2-carboxylate (**5b**) with thermal ellipsoids at 30% level.

Access to the macrocyclic quinoxaline **8** was then performed, using a three-step synthetic pathway. After treatment of trifluoroacetate salt **3** with *N,N'*-diisopropylethylamine (DIPEA), the resulting amine derivative was then engaged in a nucleophilic aromatic substitution reaction with quinoxaline **5a**, in refluxing dry tetrahydrofuran (THF) [16], to yield intermediate **6**, which underwent an intramolecular Sonogashira cross-coupling reaction, using PdCl₂(PPh₃)₂, and CuI, as catalysts, and triethylamine in refluxing THF [25],

leading to the macrocyclic quinoxaline **7**. Hydrolysis of ethyl ester **7** with potassium carbonate in 80% aqueous methanol [17] was then performed to afford the macrocyclic potassium salt **8**. The structure of this new macrocyclic quinoxaline derivative **8** was then confirmed by ¹H NMR, and HRMS analysis (see Supplementary Materials).

2.2. Protein Kinase Assays

The ability of the macrocyclic quinoxaline **8** to inhibit the in vitro enzymatic activity of human Pim-1 and Pim-2, and of a selected panel of six human off-target protein kinases (comprising DYRK1A, CDK5/p25, CDK9/CyclinT, Haspin, CK1 ϵ and GSK3 β), was evaluated, using a luminescence-based kinase assay [26]. The commercially available pan-Pim protein kinase inhibitor, SGI-1776 [27], was used as a control for the in vitro studies. As shown in Table 1, compound **8** displayed a submicromolar activity on Pim-1 and Pim-2 (IC₅₀ of 400 nM, and 100 nM, respectively) with the same level of activity on Pim-2 but a slightly decreased activity on Pim-1, in comparison to lead compound **1** and SGI-1776, the reference drug. However, the general selectivity profile of macrocycle **8** on the panel of human protein kinases studied was significantly improved in comparison to compound **1** and SGI-1776. Indeed, while compound **1** displayed low micromolar inhibition of DYRK1A and GSK3 β , and SGI-1776 potently inhibited five of the six human kinases tested (IC₅₀ values of 0.05 to 9.53 μ M), compound **8** displayed an interesting selectivity profile against the six potential off-target kinases (CDK5/p25, CDK9/CyclinT, Haspin, CK1 ϵ and GSK3 β), with IC₅₀ inhibition values > 10 μ M in every case.

Table 1. Kinase selectivity profile of compounds **1** and **8**.

Compound	Kinase Enzymatic IC ₅₀ (μ M) ^(a)							
	Pim-1	Pim-2	DYRK1A	CDK5/p25	CDK9/CyclinT	Haspin	CK1 ϵ	GSK3 β
1	0.13	0.17	2.58	>10	>10	>10	>10	2.80
8	0.40	0.10	>10	>10	>10	>10	>10	>10
SGI-1776	0.05	0.10	3.80	9.53	1.08	0.05	6.54	>10

^(a) IC₅₀ on disease-related kinase activity were calculated from dose-response curves. Each inhibitor concentration was tested in duplicate. All protein kinases used here are human. DYRK1A: dual specificity tyrosine phosphorylation regulated kinase 1A, CDK: cyclin-dependent kinase, Haspin: haploid germ cell-specific nuclear protein kinase, CK1: casein kinase 1, GSK3: glycogen synthase kinase 3.

3. Materials and Methods

All solvents were anhydrous reagents from commercial sources. Unless otherwise noted, all chemicals and reagents were obtained commercially and used without purification. Reactions were monitored by thin-layer chromatography (TLC), using pre-coated aluminum sheets silica gel 60 F254 (Merck) and an ultraviolet (UV) light at 254 and 365 nm, for the visualization. Melting points (m.p.) were determined on a Stuart capillary apparatus and are uncorrected. High-resolution mass spectra (HRMS) were performed on a Bruker maXis mass spectrometer or on a Q-Exactive mass spectrometer (Thermo Fisher Scientific, Waltham, MA USA), in positive mode with an ESI source. NMR spectra were recorded at 400 MHz (¹H), 101 MHz (¹³C) or 376 MHz (¹⁹F) on a Bruker Avance (400 MHz) spectrometer. The chemical shifts are reported in parts per million (ppm, δ) relative to residual deuterated solvent peaks. The abbreviations s = singlet, d = doublet, t = triplet, q = quadruplet, m = multiplet and bs = broad signal were used throughout.

3.1. Tert-Butyl (3-(Pent-4-ynamido)phenyl)carbamate (**2**)

To a solution of pent-4-ynoic acid (106 mg, 1.08 mmol) in dry N,N-dimethylformamide (DMF) (3 mL), under an argon atmosphere, were added 1-[Bis(dimethylamino)methylene]-1H-1,2,3-triazolo[4,5-b]pyridinium 3-oxid hexafluoro-phosphate (HATU) (680 mg, 1.79 mmol) in solution in dry DMF (3 mL) and 2,6-lutidine (207 μ L, 1.79 mmol) were added. The resulting mixture was stirred magnetically at room temperature for 10 min. Tert-butyl (3-

aminophenyl)carbamate (188 mg, 0.90 mmol) was then added, and the mixture was stirred at room temperature for 24 h. The solvent was then removed under reduced pressure, and the residue was finally purified by silica column chromatography using cyclohexane with ethyl acetate gradient (0–60%) as eluent, to give compound **2** (214 mg, 69%) as a white powder, m.p. 130 °C. ¹H NMR (400 MHz, DMSO-*d*₆) δ 9.91 (s, 1H), 9.32 (s, 1H), 7.78 (s, 1H), 7.29 (d, *J* = 8.4 Hz, 1H), 7.13 (dd, *J* = 8.4, 8.8 Hz, 1H), 7.02 (d, *J* = 8.8 Hz, 1H), 2.78 (t, *J* = 2.4 Hz, 1H), 2.50–2.40 (m, 4H), 1.47 (s, 9H). ¹³C NMR (101 MHz, DMSO-*d*₆) δ 169.2, 152.7, 139.8, 139.4, 128.7, 113.3, 113.0, 109.1, 83.7, 78.9, 71.4, 35.1, 28.1 (3 × C), 14.1. HRMS (ESI) *m/z*: [M+H]⁺ calcd for C₁₆H₂₁N₂O₃, 289.15467; found 289.15448.

3.2. 3-(Pent-4-ynamido)benzenaminium Trifluoroacetic Salt (**3**)

To a solution of compound **2** (1.20 g, 4.16 mmol) in dichloromethane (DCM) (40 mL) trifluoroacetic acid (TFA) (4 mL) was added dropwise at 0 °C. The resulting mixture was stirred magnetically at 0 °C for 30 min, and then at room temperature for 5 h. The solvent was then removed under reduced pressure, and the residue was finally purified by silica column chromatography using DCM with methanol (MeOH) gradient (0–15%) as eluent, to give compound **3** (1.19 g, 100%) as a brown oil. ¹H NMR (400 MHz, DMSO-*d*₆) δ 10.01 (s, 1H), 7.50 (s, 1H), 7.20 (dd, *J* = 8.4, 7.6 Hz, 1H), 7.12 (d, *J* = 8.4 Hz, 1H), 6.69 (d, *J* = 7.6 Hz, 1H), 4.25–3.00 (m, 3H), 2.79 (t, *J* = 2.4 Hz, 1H), 2.55–2.40 (m, 4H). ¹³C NMR (101 MHz, DMSO-*d*₆) δ 169.8, 140.2, 134.7, 130.0, 116.7, 116.3, 112.2, 83.6, 71.5, 35.2, 14.1. ¹⁹F NMR (376 MHz, DMSO-*d*₆) δ –74.1 (s).

3.3. Ethyl 5-Iodo-3-oxo-3,4-dihydroquinoxaline-2-carboxylate (**4a**) and ethyl 8-iodo-3-oxo-3,4-dihydroquinoxaline-2-carboxylate (**4b**)

A mixture of 3-iodo-1,2-phenylenediamine (1.00 g, 4.27 mmol), diethyl 2-oxomalonate (0.81 mL, 5.31 mmol), and citric acid (132 mg, 0.69 mmol) in ethanol (50 mL) was stirred magnetically at 50 °C for 3 h. Ethanol was then evaporated under reduced pressure, and the resulting residue was purified by silica column chromatography using cyclohexane with ethyl acetate gradient (0–70%) as eluent to give compound **4a** (275 mg, 19%) and its 8-iodo isomer **4b** (1.01 g, 69%) as yellow powders.

Compound **4a**: m.p. 162 °C. ¹H NMR (400 MHz, DMSO-*d*₆) δ 11.54 (bs, 1H), 8.21 (d, *J* = 6.0 Hz, 1H), 7.90 (d, *J* = 7.6 Hz, 1H), 7.24 (dd, *J* = 7.6, 6.0 Hz, 1H), 4.39 (q, *J* = 7.2 Hz, 2H), 1.33 (t, *J* = 7.2 Hz, 3H). HRMS (ESI) *m/z*: [M+H]⁺ calcd for C₁₁H₁₀IN₂O₃, 344.97306; found 344.97316.

Compound **4b**: m.p. 238 °C. ¹H NMR (400 MHz, DMSO-*d*₆) δ 12.96 (bs, 1H), 7.89 (dd, *J* = 4.4, 2.4 Hz, 1H), 7.37–7.29 (m, 2H), 4.39 (qd, *J* = 7.2, 2.0 Hz, 2H), 1.33 (td, *J* = 7.2, 2.0 Hz, 3H). HRMS (ESI) *m/z*: [M+H]⁺ calcd for C₁₁H₁₀IN₂O₃, 344.97306; found 344.97306.

3.4. Ethyl 3-Chloro-5-iodoquinoxaline-2-carboxylate (**5a**)

Method A: into a dry three-neck round bottom flask was introduced compound **4a** (100 mg, 0.29 mmol) in phosphorous oxychloride (0.96 mL) at ice bath temperature. The mixture was vigorously stirred magnetically at 0 °C for 5 min and DMF (42 μL) was then added at 0 °C and the reaction mixture was refluxed for 1 h. After cooling at 0 °C, the resulting mixture was neutralized with a 1 M sodium hydroxide aqueous solution, and extracted with ethyl acetate. The combined organic layers were washed with brine, and dried over MgSO₄, filtered, and evaporated under reduced pressure to obtain derivative **5a** (102 mg, 97%) as a yellow solid, m.p. 120 °C. ¹H NMR (400 MHz, DMSO-*d*₆) δ 8.61 (dd, *J* = 7.6, 1.2 Hz, 1H), 8.23 (dd, *J* = 8.4, 1.2 Hz, 1H), 7.75 (dd, *J* = 8.4, 7.6 Hz, 1H), 4.50 (q, *J* = 7.2 Hz, 2H), 1.39 (t, *J* = 7.2 Hz, 3H). ¹³C NMR (101 MHz, DMSO-*d*₆) δ 162.9, 144.8, 143.9, 143.0, 141.7, 139.7, 133.0, 129.9, 100.7, 62.8, 13.9. HRMS (ESI) *m/z*: [M+H]⁺ calcd for C₁₁H₉ClIN₂O₂, 362.93917; found 362.93936.

3.5. Ethyl 3-Chloro-8-iodoquinoxaline-2-carboxylate (5b)

The title compound was synthesized according to the general method A from compound **4b** (100 mg, 0.29 mmol), phosphorous oxychloride (0.96 mL) and DMF (42 μ L). Compound **5b** was obtained (94 mg, 89%) as a yellow solid, m.p. 105 °C. ^1H NMR (400 MHz, DMSO-*d*₆) δ 8.55 (dd, *J* = 7.2, 0.8 Hz, 1H), 8.10 (dd, *J* = 8.4, 0.8 Hz, 1H), 7.75 (dd, *J* = 8.4, 7.2 Hz, 1H), 4.52 (qd, *J* = 7.2, 1.6 Hz, 2H), 1.40 (td, *J* = 7.2, 1.6 Hz, 3H). ^{13}C NMR (101 MHz, DMSO-*d*₆) δ 163.4, 145.4, 144.1, 142.4, 142.2, 139.7, 134.8, 129.3, 102.9, 63.3, 14.4. HRMS (ESI) *m/z*: [M+H]⁺ calcd for C₁₁H₉ClIN₂O₂, 362.93917; found 362.93920.

3.6. Ethyl 5-Iodo-3-((3-(pent-4-ynamido)phenyl)amino)quinoxaline-2-carboxylate (6)

To a solution of trifluoroacetic salt **3** (160 mg, 0.56 mmol) and *N,N'*-diisopropylethylamine (DIPEA) (500 μ L, 2.87 mmol) in dry tetrahydrofuran (THF) (3 mL), under an argon atmosphere, was added dropwise compound **5a** (64 mg, 0.18 mmol) in solution in dry THF (1 mL). The resulting mixture was refluxed for 2 days. The solvent was then removed under reduced pressure, and the residue was finally purified by silica column chromatography using cyclohexane with ethyl acetate gradient (0–100%) as eluent to give intermediate **6** (37 mg, 41%) as a yellow powder, m.p. 127 °C. ^1H NMR (400 MHz, DMSO-*d*₆) δ 10.36 (s, 1H), 9.99 (s, 1H), 8.56 (d, *J* = 8.4 Hz, 1H), 8.38 (dd, *J* = 7.6, 1.2 Hz, 1H), 8.02 (dd, *J* = 8.0, 1.2 Hz, 1H), 7.92 (s, 1H), 7.41–7.32 (m, 2H), 7.22 (d, *J* = 8.8 Hz, 1H), 4.51 (q, *J* = 7.2 Hz, 2H), 2.82 (t, *J* = 2.4 Hz, 1H), 2.59–2.50 (m, 4H), 1.43 (t, *J* = 7.2 Hz, 3H). ^{13}C NMR (101 MHz, DMSO-*d*₆) δ 169.5, 165.2, 148.6, 142.3, 142.1, 139.5, 139.1, 135.5, 133.3, 130.2, 129.3, 127.6, 115.0, 114.3, 110.8, 98.5, 83.7, 71.5, 62.5, 35.2, 14.1, 14.0. HRMS (ESI) *m/z*: [M+H]⁺ calcd for C₂₂H₂₀IN₄O₃, 515.05746; found 515.05783.

3.7. Ethyl 6-Oxo-7,13,16,22-tetraazatetracyclo[12.6.2.1^{8,12}.0^{17,21}]tricoso-1(20),8(23),9,11,14,16,18,21-octaen-2-yne-15-carboxylate (7)

Into a sealed tube were introduced bis(triphenylphosphine) palladium (II) dichloride (PdCl₂(PPh₃)₂) (4 mg, 5.7 μ mol), copper iodide (CuI) (0.3 mg, 1.6 μ mol) and triethylamine (16 μ L, 0.12 mmol) in dry THF (3 mL), under an argon atmosphere. Then, intermediate **6** (20 mg, 39 μ mol) in dry THF (3 mL) was added dropwise, and the reaction mixture was refluxed for 16 h. The solvent was then removed under reduced pressure, and the residue was finally purified by silica column chromatography using cyclohexane with ethyl acetate gradient (0–100%) as eluent to give the macrocycle **7** (1.2 mg, 8%), as a yellow oil. *R_f* value = 0.28 (SiO₂, cyclohexane/ethyl acetate, 60/40, *v/v*). ^1H NMR (400 MHz, DMSO-*d*₆) δ 10.16 (s, 1H), 9.60 (s, 1H), 9.48 (bs, 1H), 7.97 (dd, *J* = 8.4, 0.8 Hz, 1H), 7.87 (dd, *J* = 7.2, 0.8 Hz, 1H), 7.53 (dd, *J* = 8.4, 7.2 Hz, 1H), 7.34 (t, *J* = 8.0 Hz, 1H), 7.06 (dd, *J* = 8.0, 1.6 Hz, 1H), 6.79 (dd, *J* = 8.0, 1.6 Hz, 1H), 4.50 (q, *J* = 7.2 Hz, 2H), 2.95 (t, *J* = 5.6 Hz, 2H), 2.59 (t, *J* = 5.6 Hz, 2H), 1.42 (t, *J* = 7.2 Hz, 3H). ^{13}C NMR (101 MHz, DMSO-*d*₆) δ 172.7, 165.2, 147.9, 142.6, 139.6, 139.3, 135.4, 135.0, 132.5, 129.3, 129.0, 126.1, 120.4, 119.0, 118.6, 116.8, 95.5, 78.6, 62.4, 29.0, 16.2, 14.0. HRMS (ESI) *m/z*: [M+H]⁺ calcd for C₂₂H₁₉N₄O₃, 387.14572; found 387.14516.

3.8. Potassium 6-Oxo-7,13,16,22-tetraazatetracyclo[12.6.2.1^{8,12}.0^{17,21}]tricoso-1(20),8(23),9,11,14,16,18,21-octaen-2-yne-15-carboxylate (8)

To ester **7** (1 mg, 2.6 μ mol) in aqueous methanol (80%, 2 mL), potassium carbonate (0.36 mg, 2.6 μ mol) was added and the reaction mixture was stirred magnetically at room temperature for 1 h. After cooling, MeOH was removed under reduced pressure, and the aqueous phase was washed with ethyl acetate, and evaporated under reduced pressure to yield macrocycle **8** (1 mg, 97%) as a yellow powder, m.p. > 350 °C. ^1H NMR (400 MHz, DMSO-*d*₆) δ 13.29 (s, 1H), 9.62 (s, 1H), 9.61 (bs, 1H), 7.86 (dd, *J* = 8.0, 1.2 Hz, 1H), 7.66 (d, *J* = 7.2, 1.2 Hz, 1H), 7.38 (dd, *J* = 8.0, 7.2 Hz, 1H), 7.28 (t, *J* = 8.0 Hz, 1H), 6.86 (d, *J* = 8.0, 2.0 Hz, 1H), 6.70 (dd, *J* = 8.0, 2.0 Hz, 1H), 2.94 (t, *J* = 4.8 Hz, 2H), 2.65 (t, *J* = 4.8 Hz, 2H). HRMS (ESI) *m/z*: [M+2H]⁺ calcd for C₂₀H₁₅N₄O₃, 359.11442, found 359.11401.

3.9. X-ray Data

The structure of compound **5b** was established by X-ray crystallography (Figure 2). The yellow single crystal of **5b** was obtained by slow evaporation from a methanol/chloroform solution (*v/v*: 20/80): triclinic, space group P-1, *a* = 6.6838(5) Å, *b* = 8.6592(6) Å, *c* = 10.5128(7) Å, α = 79.521(2)°, β = 89.243(2)°, γ = 86.626(2)°, *V* = 597.26 (7) Å³, *Z* = 2, δ (calcd) = 2.016 Mg.m⁻³, *FW* = 362.54 for C₁₁H₈ClIN₂O₂, *F*(000) = 348. Full crystallographic results have been deposited at the Cambridge Crystallographic Data Centre (CCDC-2262892), UK, as Supplementary Materials [28]. The data were corrected for Lorentz and polarization effects and for empirical absorption correction [29]. The structure was solved by direct methods Shelx 2013 [30] and refined using Shelx 2013 [30] suite of programs.

3.10. Protein Kinase Assays

Kinase enzymatic activities were assayed with 10 μM ATP in 384-well plates using the luminescent ADP-Glo™ assay (Promega, Madison, WI, USA), as previously described by our team [16,17], according to the recommendations of the manufacturer (see [26] for details on this method).

4. Conclusions

Taking into account our previous studies, using the biological active quinoxaline-2-carboxylic acid scaffold, we designed and synthesized a new potassium 6-oxo-7,13,16,22-tetraazatetracyclo[12.6.2.1^{8,12}.0^{17,21}]tricoso-1(20),8(23),9,11,14,16,18,21-octaen-2-yne-15-carboxylate **8** and then evaluated its anti-Pim-1/2 kinase activity. This macrocyclic quinoxaline **8** exhibited submicromolar activity on Pim-1 and Pim-2, with a significantly improved selectivity profile on the panel of human protein kinases studied in comparison to lead compound **1** and the reference drug SGI-1776. This compound could therefore represent a new attractive candidate for extending further pharmacomodulation studies and pharmacological investigations.

Supplementary Materials: ¹H NMR, ¹³C NMR, and HRMS spectra are available online.

Author Contributions: Conceptualization, C.D.-S. and C.L.; methodology, C.D.-S., C.B., M.-C.V.-M. and N.J.; investigation, C.B., S.L., C.L., C.D.-S., J.G., N.P., T.R. and S.B.; writing—original draft preparation, C.D.-S. and C.B.; writing—review and editing, C.D.-S.; supervision, C.D.-S.; project administration, C.D.-S.; funding acquisition, C.D.-S. All authors have read and agreed to the published version of the manuscript.

Funding: This work was funded by a grant from the Centre-Val de Loire Region and from the French National Research Agency under the program “Investissements d’avenir” Grant Agreement LabEx SynOrg (ANR-11-LABX-0029). The authors also thank the Cancéropôle Grand Ouest (3MC network—Marine Molecules, Metabolism and Cancer), GIS IBI SA (Infrastructures en Biologie Santé et Agronomie) and Biogenouest (Western France life science and environment core facility network) for supporting the KISSf screening facility. C. Blouet thanks the Centre-Val de Loire Region and the LabEx SynOrg for her PhD fellowship.

Data Availability Statement: Not applicable.

Acknowledgments: The authors would like to thank Cyril Colas from the “Fédération de Recherche” ICOA/CBM (FR2708) and the «Plateforme Scientifique et Technique Analyses des Systèmes Biologiques» (PST-ASB), for HRMS analysis, and Cécile Croix, from CEPR, for NMR spectrometry and technical support.

Conflicts of Interest: The authors declare no conflict of interest.

References

1. Mochizuki, T.; Kitanaka, C.; Noguchi, K.; Muramatsu, T.; Asai, A.; Kuchino, Y. Physical and Functional Interactions between Pim-1 Kinase and Cdc25A Phosphatase. Implications for the Pim-1-Mediated Activation of the c-Myc Signaling Pathway. *J. Biol. Chem.* **1999**, *274*, 18659–18666. [[CrossRef](#)] [[PubMed](#)]

2. Bachmann, M.; Kosan, C.; Xing, P.X.; Montenarh, M.; Hoffmann, I.; Möröy, T. The Oncogenic Serine/Threonine Kinase Pim-1 Directly Phosphorylates and Activates the G2/M Specific Phosphatase Cdc25C. *Int. J. Biochem. Cell Biol.* **2006**, *38*, 430–443. [[CrossRef](#)] [[PubMed](#)]
3. Theo Cuyppers, H.; Selten, G.; Quint, W.; Zijlstra, M.; Maandag, E.R.; Boelens, W.; van Wezenbeek, P.; Melief, C.; Berns, A. Murine Leukemia Virus-Induced T-Cell Lymphomagenesis: Integration of Proviruses in a Distinct Chromosomal Region. *Cell* **1984**, *37*, 141–150. [[CrossRef](#)] [[PubMed](#)]
4. Narlik-Grassow, M.; Blanco-Aparicio, C.; Carnero, A. The PIM Family of Serine/Threonine Kinases in Cancer. *Med. Res. Rev.* **2014**, *34*, 136–159. [[CrossRef](#)]
5. Toth, R.K.; Warfel, N.A. Targeting PIM Kinases to Overcome Therapeutic Resistance in Cancer. *Mol. Cancer Ther.* **2021**, *20*, 3–10. [[CrossRef](#)] [[PubMed](#)]
6. Keane, N.A.; Reidy, M.; Natoni, A.; Raab, M.S.; O'Dwyer, M. Targeting the Pim Kinases in Multiple Myeloma. *Blood Cancer J.* **2015**, *5*, e325. [[CrossRef](#)]
7. Amson, R.; Sigaux, F.; Przedborski, S.; Flandrin, G.; Givol, D.; Telerman, A. The Human Protooncogene Product P33pim Is Expressed during Fetal Hematopoiesis and in Diverse Leukemias. *Proc. Natl. Acad. Sci. USA* **1989**, *86*, 8857–8861. [[CrossRef](#)]
8. Koblisch, H.; Li, Y.L.; Shin, N.; Hall, L.; Wang, Q.; Wang, K.; Covington, M.; Marando, C.; Bowman, K.; Boer, J.; et al. Preclinical Characterization of INCB053914, a Novel Pan-PIM Kinase Inhibitor, Alone and in Combination with Anticancer Agents, in Models of Hematologic Malignancies. *PLoS ONE* **2018**, *13*, e0199108. [[CrossRef](#)]
9. Czardybon, W.; Windak, R.; Gołas, A.; Gałezowski, M.; Sabiniaż, A.; Dolata, I.; Salwińska, M.; Guzik, P.; Zawadzka, M.; Gabor-Worwa, E.; et al. A Novel, Dual Pan-PIM/FLT3 Inhibitor SEL24 Exhibits Broad Therapeutic Potential in Acute Myeloid Leukemia. *Oncotarget* **2018**, *9*, 16917–16931. [[CrossRef](#)]
10. Bellon, M.; Nicot, C. Targeting Pim Kinases in Hematological Cancers: Molecular and Clinical Review. *Mol. Cancer* **2023**, *22*, 18. [[CrossRef](#)]
11. Qu, Y.; Zhang, C.; Du, E.; Wang, A.; Yang, Y.; Guo, J.; Wang, A.; Zhang, Z.; Xu, Y. Pim-3 Is a Critical Risk Factor in Development and Prognosis of Prostate Cancer. *Med. Sci. Monit.* **2016**, *22*, 4254–4260. [[CrossRef](#)] [[PubMed](#)]
12. Mikkers, H.; Nawijn, M.; Allen, J.; Brouwers, C.; Verhoeven, E.; Jonkers, J.; Berns, A. Mice Deficient for All PIM Kinases Display Reduced Body Size and Impaired Responses to Hematopoietic Growth Factors. *Mol. Cell. Biol.* **2004**, *24*, 6104–6115. [[CrossRef](#)] [[PubMed](#)]
13. An, N.; Kraft, A.S.; Kang, Y. Abnormal Hematopoietic Phenotypes in Pim Kinase Triple Knockout Mice. *J. Hematol. Oncol.* **2013**, *6*, 12. [[CrossRef](#)] [[PubMed](#)]
14. Kumar, A.; Mandiyan, V.; Suzuki, Y.; Zhang, C.; Rice, J.; Tsai, J.; Artis, D.R.; Ibrahim, P.; Bremer, R. Crystal Structures of Proto-Oncogene Kinase Pim1: A Target of Aberrant Somatic Hypermutations in Diffuse Large Cell Lymphoma. *J. Mol. Biol.* **2005**, *348*, 183–193. [[CrossRef](#)] [[PubMed](#)]
15. Bullock, A.N.; Russo, S.; Amos, A.; Pagano, N.; Bregman, H.; Debreczeni, J.É.; Lee, W.H.; von Delft, F.; Meggers, E.; Knapp, S. Crystal Structure of the PIM2 Kinase in Complex with an Organoruthenium Inhibitor. *PLoS ONE* **2009**, *4*, e7112. [[CrossRef](#)] [[PubMed](#)]
16. Oyallon, B.; Brachet-Botineau, M.; Logé, C.; Robert, T.; Bach, S.; Ibrahim, S.; Raoul, W.; Croix, C.; Berthelot, P.; Guillon, J.; et al. New Quinoxaline Derivatives as Dual Pim-1/2 Kinase Inhibitors: Design, Synthesis and Biological Evaluation. *Molecules* **2021**, *26*, 867. [[CrossRef](#)]
17. Oyallon, B.; Brachet-Botineau, M.; Logé, C.; Bonnet, P.; Souab, M.; Robert, T.; Ruchaud, S.; Bach, S.; Berthelot, P.; Gouilleux, F.; et al. Structure-Based Design of Novel Quinoxaline-2-Carboxylic Acids and Analogues as Pim-1 Inhibitors. *Eur. J. Med. Chem.* **2018**, *154*, 101–109. [[CrossRef](#)]
18. Liang, Y.; Fang, R.; Rao, Q. An Insight into the Medicinal Chemistry Perspective of Macrocyclic Derivatives with Antitumor Activity: A Systematic Review. *Molecules* **2022**, *27*, 2837. [[CrossRef](#)]
19. Basit, S.; Ashraf, Z.; Lee, K.; Latif, M. First Macrocyclic 3rd-Generation ALK Inhibitor for Treatment of ALK/ROS1 Cancer: Clinical and Designing Strategy Update of Lorlatinib. *Eur. J. Med. Chem.* **2017**, *134*, 348–356. [[CrossRef](#)]
20. Verstovsek, S.; Komrokji, R.S. A Comprehensive Review of Pacritinib in Myelofibrosis. *Futur. Oncol.* **2015**, *11*, 2819–2830. [[CrossRef](#)]
21. Bryden, F.; Martin, C.; Letast, S.; Lles, E.; Viéitez-Villemin, I.; Rousseau, A.; Colas, C.; Brachet-Botineau, M.; Allard-Vannier, E.; Larbouret, C.; et al. Impact of Cathepsin B-Sensitive Triggers and Hydrophilic Linkers on: In Vitro Efficacy of Novel Site-Specific Antibody-Drug Conjugates. *Org. Biomol. Chem.* **2018**, *16*, 1882–1889. [[CrossRef](#)] [[PubMed](#)]
22. Shendage, D.M.; Fröhlich, R.; Haufe, G. Highly Efficient Stereoconservative Amidation and Deamidation of α -Amino Acids. *Org. Lett.* **2004**, *6*, 3675–3678. [[CrossRef](#)] [[PubMed](#)]
23. Mahesh, R.; Dhar, A.K.; Tara Sasank, T.V.N.V.; Thirunavukkarasu, S.; Devadoss, T. Citric Acid: An Efficient and Green Catalyst for Rapid One Pot Synthesis of Quinoxaline Derivatives at Room Temperature. *Chin. Chem. Lett.* **2011**, *22*, 389–392. [[CrossRef](#)]
24. Mahesh, R.; Devadoss, T.; Dhar, A.K.; Venkatesh, S.M.; Mundra, S.; Pandey, D.K.; Bhatt, S.; Jindal, A.K. Ligand-Based Design, Synthesis, and Pharmacological Evaluation of 3-Methoxyquinoxalin-2-Carboxamides as Structurally Novel Serotonin Type-3 Receptor Antagonists. *Arch. Pharm.* **2012**, *345*, 687–694. [[CrossRef](#)] [[PubMed](#)]
25. Hussain, A.; Rao, M.; Sharma, D.K.; Tripathi, A.K.; Singh, B.; Mukherjee, D. Synthesis of Carbohydrate Fused Chiral Macrocyclic Benzolactones through Sonogashira Reaction. *RSC Adv.* **2013**, *3*, 19899–19904. [[CrossRef](#)]

26. Zegzouti, H.; Zdanovskaia, M.; Hsiao, K.; Goueli, S.A. ADP-Glo: A Bioluminescent and Homogeneous Adp Monitoring Assay for Kinases. *Assay Drug Dev. Technol.* **2009**, *7*, 560–572. [[CrossRef](#)]
27. Blanco-Aparicio, C.; Carnero, A. Pim Kinases in Cancer: Diagnostic, Prognostic and Treatment Opportunities. *Biochem. Pharmacol.* **2013**, *85*, 629–643. [[CrossRef](#)]
28. Supplementary X-ray Crystallographic Data: Cambridge Crystallographic Data Centre, University Chemical Lab, Lensfield Road, Cambridge, CB2 1EW, UK. Available online: <https://www.ccdc.cam.ac.uk/> (accessed on 15 May 2023).
29. Sheldrick, G.M. *SADABS*; University of Göttingen: Göttingen, Germany, 1996.
30. Sheldrick, G.M. A short history of SHELX. *Acta Crystallogr. Sect. A* **2008**, *64*, 112–122. [[CrossRef](#)]

Disclaimer/Publisher’s Note: The statements, opinions and data contained in all publications are solely those of the individual author(s) and contributor(s) and not of MDPI and/or the editor(s). MDPI and/or the editor(s) disclaim responsibility for any injury to people or property resulting from any ideas, methods, instructions or products referred to in the content.